Inorganic Chemistry

Article

pubs.acs.org/IC

Cyclometalated Ruthenium Oligomers with 2,3-Di(2-pyridyl)-5,6-diphenylpyrazine: A Combined Experimental, Computational, and Comparison Study with Noncyclometalated Analogous

Si-Hai Wu,[†,‡] Stephen E. Burkhardt,[§,¶] Yu-Wu Zhong,*[,†] and Héctor D. Abruña*[,§]

[†]Beijing National Laboratory for Molecular Sciences, CAS Key Laboratory of Photochemistry, Institute of Chemistry, Chinese Academy of Sciences, Beijing 100190, People's Republic of China

[‡]University of Chinese Academy of Sciences, Beijing 100049, People's Republic of China

[§]Baker Laboratory, Department of Chemistry and Chemical Biology, Cornell University, Ithaca, New York 14853-1301, United States

Supporting Information

ABSTRACT: Recent investigations on polypyridine transition-metal complexes as potential molecular wires have provided new impetus for these long-studied and well-established systems. Using bridging ligands 2,3-di(2-pyridyl)-5,6-diphenylpyrazine (dpdpz) and 2,3,5,6-tetrakis(2-pyridyl)-pyrazine (tppz), a tetrametallic cyclometalated ruthenium complex has been prepared and characterized, with each metal having one Ru−C bond. The electronic properties of this complex and two known monoruthenium and diruthenium complexes with dpdpz (DPDPZ series) were probed by electrochemical and spectroscopic techniques and compared to the previously reported tppz-based noncyclometalated ruthenium complexes (TPPZ series). The frontier orbital energy levels and electronic structures of the two series have been characterized by density functional theory (DFT) calculations. In accordance with the experimental results, these studies suggest that the DPDPZ series oligomers generally have a narrower energy gap relative to the TPPZ series. In addition, the large energy density of states in longer oligomers suggests the possibility of band-type conduction. The DPDPZ series exhibits red-shifted light absorption with enhanced intensity relative to the TPPZ series congeners. Time-dependent DFT computations have been performed to rationalize the electronic absorption of the DPDPZ series. Oxidative spectroelectrochemical measurements of the DPDPZ tetrametallic complex indicate the presence of intervalence charge-transfer transitions among ruthenium sites.

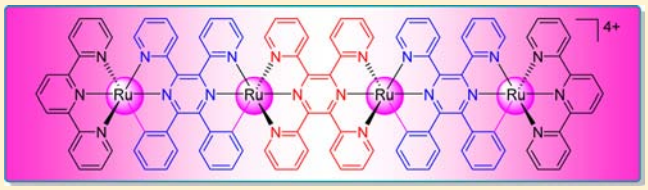

INTRODUCTION

One-dimensional conjugated materials with excellent charge-transport properties have been the focus of many research activities.[1] Compared to conjugated organic polymers,[2] multinuclear inorganic transition-metal complexes offer advantages such as well-defined geometries (controlled by bridging ligands and coordination chemistry of metals) and appealing electrochemical and photophysical properties.[3] They exhibit a high degree of electronic coupling and are most attractive for the generation of highly conductive one-dimensional molecular wires because of their extended π conjugation and ability to mediate electron transfer through multiple redox states of transition metals. Accordingly, many efforts have been devoted to the design and synthesis of new coordination oligomers and polymers toward applications such as molecular electronics,[4] nonlinear optics,[5] electrochromism,[6] and photovoltaics.[7]

The physical properties of multinuclear coordination complexes strongly depend on the bridging ligand used.[8] A suitable bridging ligand will allow optimal orbital overlap between metals and organic ligands and thus give rise to extensive delocalization, which is critical for effective charge transport along the molecular chains. We recently reported that 2,3-di(2-pyridyl)-5,6-diphenylpyrazine (dpdpzH_2; Figure 1) displayed rich coordination chemistry with various transition metals such as ruthenium,[9] platinum,[10] and rhenium[11] to yield a number of mononuclear and dinuclear complexes with interesting electrochemical and spectroscopic properties. This ligand can bind to a metal center either in a C^N^N tridentate or a N^N bidentate coordination mode depending on the metal components involved. We are particularly interested in using dpdpzH_2 and other bridging ligands[12] for the construction of one-dimensional cyclometalated coordination polymers. Compared to conventional noncyclometalated complexes sur-

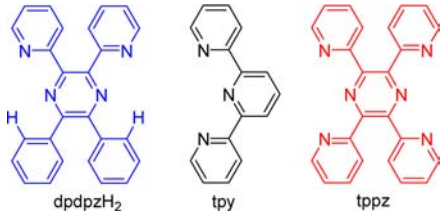

Figure 1. Polypyridine ligands.

Received: September 9, 2012
Published: December 4, 2012

   dx.doi.org/10.1021/ic3019666 | *Inorg. Chem.* 2012, 51, 13312−13320

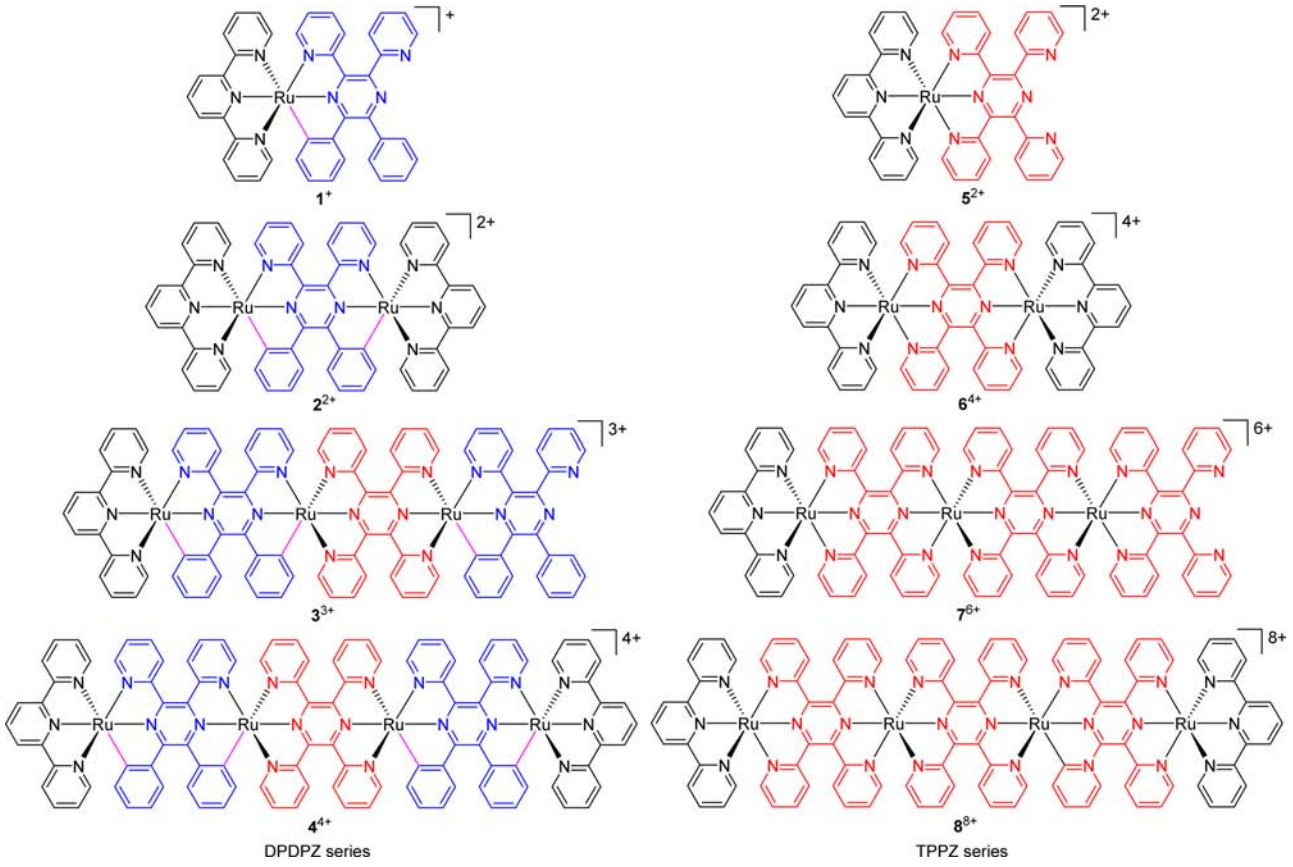

Figure 2. Compounds studied in this paper. Counteranions are $[PF_6^-]$.

rounded by neutral polyazine ligands, cyclometalated ruthenium complexes[13] contain at least one anionic ligand that binds to the metal center with a Ru−C bond to form a chelate ring. This feature makes cyclometalated ruthenium complexes attractive for solar cell applications[14] and mixed-valence chemistry[12,15] thanks to the strong orbital overlap between the metal site and cyclometalating ligand. However, cyclometalated ruthenium oligomers with more than two metal centers have not been documented, to the best of our knowledge.

We present in this paper a combined experimental and computational study of ruthenium oligomers with the bis-deprotonated form of $dpdpzH_2$ (dpdpz). On the experimental side, a tetraruthenium cyclometalated complex $[Ru_4(tpy)_2(dpdpz)_2(tppz)]^{4+}$ [$\mathbf{4}^{4+}$; tpy = 2,2′;6′,2″-terpyridine, tppz = 2,3,5,6-tetrakis(2-pyridyl)pyrazine; Figure 2] has been synthesized and studied by electrochemical and spectroscopic analysis, in addition to the previously reported monometallic complex $[Ru(tpy)(dpdpzH)]^+$ ($\mathbf{1}^+$, dpdpH is the mono-deprotonated form of $dpdpzH_2$) and dimetallic complex $[Ru_2(tpy)_2(dpdpz)]^{2+}$ ($\mathbf{2}^{2+}$).[9] On the computational side, density functional theory (DFT) calculations have been performed on $\mathbf{1}^+$, $\mathbf{2}^{2+}$, and $\mathbf{4}^{4+}$ and trimetallic complex $[Ru_3(tpy)(dpdpz)(tppz)(dpdpzH)]^{3+}$ ($\mathbf{3}^{3+}$), referred to as the DPDPZ series. In addition, time-dependent DFT (TDDFT) calculations have been performed on $\mathbf{1}^+$, $\mathbf{2}^{2+}$, and $\mathbf{4}^{4+}$. All of these experimental and computational results are compared with those of another series of noncyclometalated complexes $\mathbf{5}^{2+}$, $\mathbf{6}^{4+}$, $\mathbf{7}^{6+}$, and $\mathbf{8}^{8+}$ bridged by tppz (Figure 2, the TPPZ series).[16]

RESULTS AND DISCUSSION

Synthesis. The syntheses of ligand $dpdpzH_2$ and complexes $\mathbf{1}^+$ and $\mathbf{2}^{2+}$ have been reported previously.[9] Using a similar method for the synthesis of cyclometalated ruthenium complexes,[9,15] the tetrametallic complex $[\mathbf{4}](PF_6)_4$ was obtained in 19% yield from the reaction of $[Cl_3Ru(tppz)RuCl_3]$[17] with 2.5 equiv of the monometallic complex $\mathbf{1}^+$ in the presence of AgOTf and 4 Å molecular sieves, followed by anion exchange of KPF_6. The synthesis and purification of $\mathbf{4}^{4+}$ proved much more difficult than those of $\mathbf{1}^+$ and $\mathbf{2}^{2+}$ because of the decreased solubility and increased polarity with increasing oligomer length. The presence of 4 Å molecular sieves was found to be beneficial for transformation, which is believed to help remove a small amount of water present in the solvent. The matrix-assisted laser desorption ionization (MALDI) mass spectrometry (MS) spectrum shows signals with isotope patterns corresponding to sequential losses of PF_6 anions of $[\mathbf{4}](PF_6)_4$ (2463.4, 2317.5, 2172.6, and 2026.7 D; Figure 3). The ^1H NMR signals of $[\mathbf{4}](PF_6)_4$ cannot be clearly assigned (Figure S1 in the Supporting Information, SI) possibly because of the presence of different stereoisomers. However, the purity of the sample was proven by microanalysis data.

Electrochemical Studies. As has been reported earlier,[9] complex $\mathbf{1}^+$ shows an anodic redox couple at +0.67 V and complex $\mathbf{2}^{2+}$ displays two waves at +0.65 and +0.84 V vs Ag/AgCl. These peaks are assigned to the ruthenium(II/III) processes with possibly some involvement of oxidation of the cyclometalating ligand.[13,14] This assignment is supported by the theoretical calculations shown below. The potentials of these waves are much less positive than those of the ruthenium(II/III) processes of the TPPZ series complexes (Table 1) because

dx.doi.org/10.1021/ic3019666 | Inorg. Chem. 2012, 51, 13312−13320

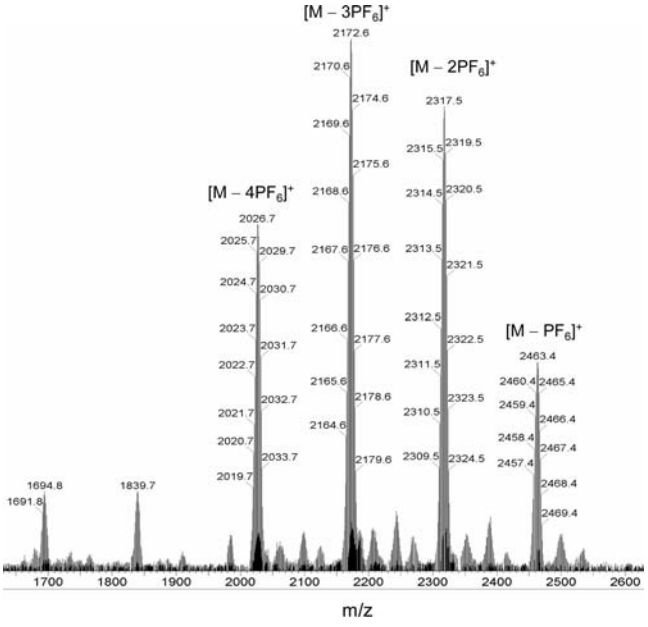

Figure 3. MALDI MS spectrum of $[\mathbf{4}](PF_6)_4$ showing signals corresponding to sequential losses of PF_6 anions.

of the presence of a σ-donating anionic carbon ligand in the cyclometalated complexes. Figure 4 shows the cyclic voltammogram (CV) and differential pulse voltammogram (DPV) of the tetraruthenium complex $\mathbf{4}^{4+}$ with $[^nBu_4N](ClO_4)$ as the supporting electrolyte. The anodic CV shows some ill-defined waves. However, the corresponding DPV can be deconvoluted into three peaks (+0.68, +0.79, and +1.01 V vs Ag/AgCl) with a 1:2:1 intensity ratio. This is in accordance with the oxidation of four ruthenium centers of $\mathbf{4}^{4+}$. The central ruthenium metals are sandwiched between two electron-withdrawing metal components. Thus, one of the terminal ruthenium sites is believed to be oxidized first, and the fourth redox couple is likely associated with one central ruthenium site. The splitting of these ruthenium(II/III) waves suggests the presence of metal–metal electronic coupling among metals. The first cathodic wave of $\mathbf{4}^{4+}$ occurs at −0.59 V. As deduced from the electrochemical data, the potential difference between the first oxidation and first reduction waves (ΔE_{echem}) of $\mathbf{4}^{4+}$ is 1.27 eV, which is much smaller than those of $\mathbf{1}^{+}$ and $\mathbf{2}^{2+}$ (Table 1). Recently, it has been shown that improved electrochemical signals can be achieved using electrolytes with weakly coordinating anions.[18] The anodic CV and DPV of $\mathbf{4}^{4+}$ in the

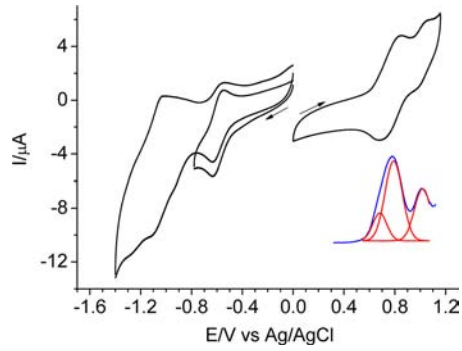

Figure 4. CV (black lines) and DPV (blue line) of $[\mathbf{4}](PF_6)_2$ in 0.1 M Bu_4NClO_4/CH_3CN. Red lines show the Gaussian-fitted DPV curves. Conditions for DPV: scan rate = 20 mV/s, pulse amplitude = 10 mV, pulse width = 50 ms, and pulse period = 200 ms.

presence of $[^nBu_4N][B(C_6F_5)_4]$[19] were then tested. However, they did not significantly improve the resolution of these peaks (Figure S2 in the SI).

The electrochemical data of the ruthenium oligomers of the DPDPZ and TPPZ series are summarized in Table 1. In comparison, the ΔE_{echem} values of the DPDPZ series are generally smaller than those of the TPPZ congeners. While experimental data can probe the electronic levels of these complexes, molecular electronics applications may also require that the electron density be (de)localized over specific functional moieties. Additionally, the synthesis and purification of coordination complexes become much more challenging with longer oligomers. For example, in the present study, the synthesis of the triruthenium complex $\mathbf{3}^{3+}$ in the DPDPZ series has not been attempted because of the synthetic difficulties in accessing the asymmetric structure of such a molecule. Computational studies are of great interest and importance for elucidating details about the electronic structure and topology of these complexes before moving on to elaborate molecular conductance experiments. Moreover, the information gained from theoretical studies would augment the electrochemical data to complete the observed trends. We describe below some preliminary computational studies on the frontier orbital energy levels of the two series and the geometric and electronic structures of the DPDPZ series.

DFT Computations. Selection of an appropriate computational method is made difficult by the high charges on the longer oligomers. Previous studies on the TPPZ oligomers have demonstrated that, in the absence of screening, the energy levels are subject to artificial compression, the so-called

Table 1. Electrochemical and DFT-Computed Data

				DFT		
series	compound	formal potential (V)[a]	ΔE_{echem}[b] (eV)	HOMO (V)	LUMO (V)	ΔE_{gap} (eV)
DPDPZ	$[Ru(tpy)(dpdpzH)]^+$ ($\mathbf{1}^+$)	+0.67, −1.33, −1.71	2.00	−5.60	−2.73	2.88
	$[Ru_2(tpy)_2(dpdpz)]^{2+}$ ($\mathbf{2}^{2+}$)	+0.65, +0.84, −1.03, −1.43	1.68	−5.67	−3.29	2.38
	$[Ru_3(tpy)(dpdpz)(tppz)(dpdpzH)]^{3+}$ ($\mathbf{3}^{3+}$)			−5.86	−3.95	1.91
	$[Ru_4(tpy)_2(dpdpz)_2(tppz)]^{4+}$ ($\mathbf{4}^{4+}$)	+0.68, +0.79, +1.01, −0.59	1.27	−5.90	−4.04	1.86
TPPZ[c]	$[Ru(tpy)(tppz)]^{2+}$ ($\mathbf{5}^{2+}$)	+1.50, −0.95, −1.40	2.45	−6.71	−3.48	3.24
	$[Ru_2(tpy)_2(tppz)]^{4+}$ ($\mathbf{6}^{4+}$)	+1.40, +1.71, −0.39, −0.86	1.79	−7.31	−4.78	2.54
	$[Ru_3(tpy)(tppz)_3]^{6+}$ ($\mathbf{7}^{6+}$)			−7.45	−5.11	2.34
	$[Ru_4(tpy)_2(tppz)_3]^{8+}$ ($\mathbf{8}^{8+}$)	+1.07, −0.20	1.27	−7.69	−5.38	2.31

[a]Unless otherwise noted, the potentials are reported as the $E_{1/2}$ value versus Ag/AgCl. [b]The potential difference between the first oxidation and first reduction waves. [c]See refs 16c and 16h.

dx.doi.org/10.1021/ic3019666 | Inorg. Chem. 2012, 51, 13312–13320

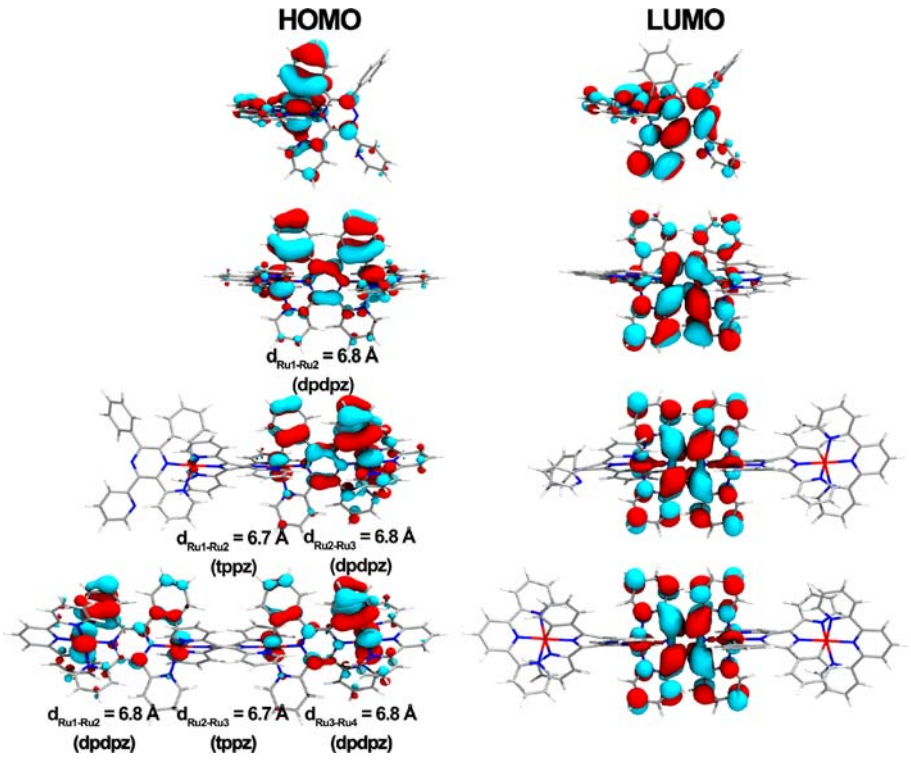

Figure 5. DPDPZ series structures ($\mathbf{1}^{+}$, $\mathbf{2}^{2+}$, $\mathbf{3}^{3+}$, and $\mathbf{4}^{4+}$ from the top). Left column: isodensity plots of HOMO orbitals. Right column: isodensity plots of LUMO orbitals. The phenyl rings of the dpdpz ligand are positioned above the central metal−metal axis. All orbitals have been computed at an isovalue of 0.02 e/bohr^3. Ru−Ru lengths are also indicated in the left column.

"charging penalty".[16h,20] The same studies have also noted that the screening provided by solvent models is not adequate to fully describe the experimental results, specifically the decrease in the oxidation potential with increasing oligomer length. In the absence of an efficient screening method that addresses the above issues, which may include counterions as well as solvent, we based the choice of method on the correct reproduction of experimental trends in highest occupied molecular orbital (HOMO)−lowest unoccupied molecular orbital (LUMO) gaps (ΔE_{gap}) for the TPPZ and DPDPZ series and a minimization of the decreasing trend in HOMO energy levels (vertical ionization energy). The computed energy levels and values of ΔE_{gap} are presented in Table 1.

The structures and isodensity plots of the HOMOs and LUMOs of the entire DPDPZ series, evaluated computationally, are shown in Figure 5. The geometry along the growth axis of the DPDPZ wires displays a helical structure similar to that seen in previously studied TPPZ series oligomers (Figure S3 in the SI). In the dimetallic complex $\mathbf{2}^{2+}$, the pyrazine N−C−C−N dihedral angles along the phenyl- and pyridyl-substituted carbon atoms are 22.5° and 20.5°, respectively. Likewise, distances between the ruthenium centers in the DPDPZ series do not differ substantially from the analogous TPPZ oligomers. The Ru−Ru distances across the tppz and dpdpz bridging ligands are 6.7 and 6.8 Å, respectively. Additionally, because of Ru−C bonds, which are shorter than the analogous Ru−N bonds, the DPDPZ series oligomers display deviations from linearity along the *c* axis (Figure S3 in the SI). This is most evident in the tetrametallic complex $\mathbf{4}^{4+}$. These calculated structures are in agreement with reported X-ray structures of tppz-bridged multimetallic complexes. For example, the trimetallic complex [ClPt(tppz)Ru(tppz)PtCl](PF$_6$)$_4$ reported by Brewer has a Pt−Ru distance of 6.55 Å and two pyrazine N−C−C−N dihedral angles of 21.6 and 18.7°.[21] The tppz-bridged diruthenium complex *cis*-[Cl(dmb)Ru(tppz)Ru(dmb)-Cl](PF$_6$)$_2$ (dmb = 4,4′-dimethyl-2,2′-bipyridine) has a Ru−Ru distance of 6.558 Å.[17]

The effects of cyclometalation are apparent in the frontier molecular orbitals. The computed HOMO has a significant character of metal d orbitals. This can be easily rationalized within the framework of a d^6 metal in an octahedral field and can be observed qualitatively via the orbital contours (Figure 5). The Mulliken population analysis also places large coefficients on the metal t_{2g} orbitals. However, there is also significant HOMO electron density on the dpdpz−phenyl rings, a feature that is absent in the TPPZ series oligomers. This has been previously reported with regard to cyclometalated ruthenium complexes.[12−15,22] The LUMO orbitals are largely ligand-based π^* orbitals. In the cases of $\mathbf{3}^{3+}$ and $\mathbf{4}^{4+}$, the LUMOs are dominated by the tppz ligand, which suggests that the first cathodic redox wave of $\mathbf{4}^{4+}$ in Figure 4 is associated with the tppz reduction.

Because of equilibration with the Fermi energy of the electrodes, a smaller ΔE_{gap} would require smaller biases for electronic conduction in a two-terminal setting. In this context, larger HOMO−LUMO gaps suggest greater geometric free-energy changes upon oxidation or reduction, and these can, in turn, be viewed as a kinetic barrier to electronic conduction.[23] In the limit of an infinite conjugation length,[24] a plot of the reciprocal oligomer length versus ΔE_{gap} allows extrapolation to ΔE_{gap} for infinite-length polymers (Figure 6). The theoretical extrapolated gap of the DPDPZ series is expected to be ∼1.5 eV, while for the TPPZ series, it is expected to converge to ∼1.9 eV.

As shown in Figure 6, the linear fit of the TPPZ series electrochemical data has a steeper slope than that of the

dx.doi.org/10.1021/ic3019666 | *Inorg. Chem.* 2012, 51, 13312−13320

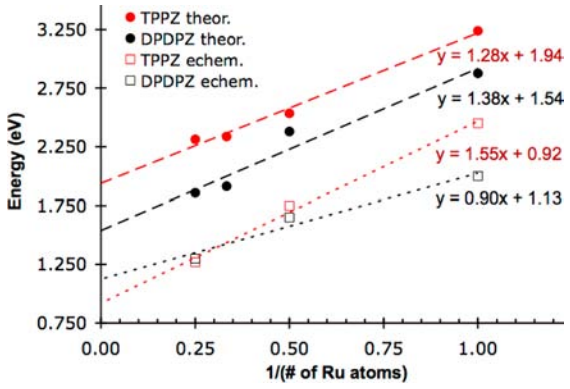

Figure 6. Plot of $1/n$ versus electrochemical potential difference ΔE_{echem} and theoretical ΔE_{gap} with linear regression for the TPPZ and DPDPZ series oligomers. The intercept is an indication of ΔE_{gap} for an infinite-length chain.

DPDPZ series. However, the slopes of the linear fit applied to both theoretical series are comparable. This would suggest that delocalization is approximately the same for both series. However, upon closer inspection, the greatest drop in ΔE_{gap} occurs between the DPDPZ dimetallic and trimetallic complexes. This corresponds to the addition of a third metal atom *and a tppz ligand* to the DPDPZ series oligomer. It is likely that the addition of a tppz ligand introduces a lower-energy LUMO state into the DPDPZ trimetallic complex. Although electrochemical data for this complex are not available, this conclusion is consistent with the experimental data, where the first reduction for the DPDPZ tetramer is positively shifted by 440 mV relative to the dimetallic complex. In the TPPZ series, the first reduction of the tetrametallic complex is positively shifted by only 190 mV relative to the dimetallic complex. Finally, the orbital contours also support localization of the LUMO on the tppz ligand in n = 3 and 4 DPDPZ oligomers. This suggests that extrapolation, based on the electrochemical data, is not complete without the data for the trimetallic species. We conjecture from the theoretical data that inclusion of the trimetallic complex would alter the slope of the electrochemical extrapolation. In other words, the slope of the linear fit applied to the electrochemical data for the DPDPZ series is artificially small because of the absence of data for the trimetallic complex.

Characteristics of molecular conductivity have also been extended to the topology of molecular orbitals, specifically the LUMO orbital, which may be the initially populated orbital when an external potential is applied across the molecule by macroscopic electrodes.[25] The LUMOs are highly delocalized across the TPPZ ligand. By analogy to the HOMO of the tetrametallic complex, which has regions of high density on both of the DPDPZ ligands, the LUMO would be expected to further delocalize onto additional TPPZ ligands as the length of the wire increases. Previously modeled TPPZ series oligomers with up to n = 8 have shown LUMO delocalization across several repeat units. In studies where TPPZ was utilized as the capping ligand, the calculated LUMO was delocalized onto the terminal ligand.[16h]

The significant electronic delocalization in these species also gives rise to a high density of states. A large energy density of states should facilitate electron transfer by presenting near-degenerate or overlapping states along the axis of growth (conduction) in both oxidized (p-doped) and reduced (n-doped) forms of the wire. Figure 7 displays the significant increases in the energy density of states with increasing

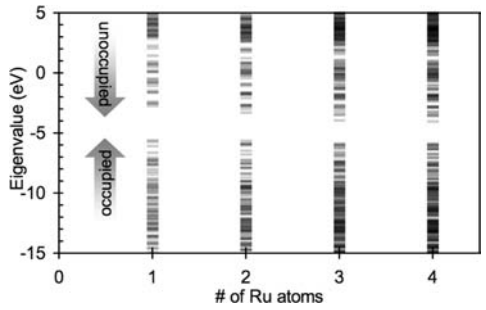

Figure 7. Plot of DFT eigenvalues versus number of ruthenium atoms for the DPDPZ series. This plot displays the increase in the energy density of states with the oligomer length. The plot suggests that band-type conduction may be possible in these types of oligomers.

oligomer length. This suggests the formation of band-type electronic structure and the possibility of band conduction. In fact, previous calculations have also shown that the reorganization energy changes associated with the reduction of TPPZ oligomers are quite small,[16h] a result that is consistent with the semiconductor behavior.

Spectroscopic Studies and TDDFT Calculations. The electronic absorption spectra of $\mathbf{1}^{+}$, $\mathbf{2}^{2+}$, and $\mathbf{4}^{4+}$ are displayed in Figure 8. Absorption in the ultraviolet (UV) region is due to

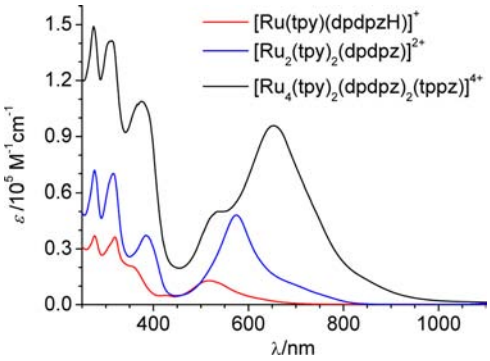

Figure 8. Electronic absorption spectra of $\mathbf{1}^{+}$ (red line), $\mathbf{2}^{2+}$ (blue line), and $\mathbf{4}^{4+}$ (black line) in CH_3CN.

intraligand $\pi-\pi^*$ excitation. The intense and broad bands in the visible to near-IR (NIR) region are ascribed to the metal-to-ligand charge-transfer (MLCT) transitions. As the oligomer length increases, the MLCT maximum shifts bathochromically (515, 574, and 651 nm for $\mathbf{1}^{+}$, $\mathbf{2}^{2+}$, and $\mathbf{4}^{4+}$, respectively). Apparently, the tetraruthenium complex displays much enhanced light absorptivity. The low-energy edge of the absorption spectrum of $\mathbf{4}^{4+}$ extends into the NIR region. A comparison of the absorption spectra of $\mathbf{2}^{2+}$, $\mathbf{4}^{4+}$, $\mathbf{6}^{4+}$, and $\mathbf{8}^{8+}$ is given in Figure S4 in the SI, which indicates that the DPDPZ series complexes exhibit red-shifted MLCT transitions with enhanced intensity relative to the corresponding TPPZ series complexes with the same metal atom numbers.

To gain insight into the nature of the MLCT absorption of the DPDPZ series, TDDFT calculations have been performed on the above DFT-optimized structures of $\mathbf{1}^{+}$, $\mathbf{2}^{2+}$, and $\mathbf{4}^{4+}$ using the same level of theory. Predicted electronic transitions are displayed in Figure S5 in the SI and delineated in Table S1

dx.doi.org/10.1021/ic3019666 | *Inorg. Chem.* 2012, 51, 13312−13320

in the SI. Frontier orbitals involved in these transitions are shown in Figures S6−S10 in the SI. TDDFT-predicted excitations are at slightly higher energies relative to the experimentally obtained spectra. However, the shapes of the predicted excitations correlate well with the experimental data. The absorption peak at 515 nm of $\mathbf{1}^{+}$ is mainly associated with the S_9 excitation (HOMO−2 → LUMO), which is a result of the MLCT transitions targeted at the dpdpz ligand. However, some amount of tpy-associated MLCT transitions is also involved (e.g., S_7 excitation of the HOMO−1 → LUMO+2 character). The low-energy edge absorption of $\mathbf{1}^{+}$ is dominated by excitations from the HOMO (S_1 and S_3 excitations). The sharp absorption peak of $\mathbf{2}^{2+}$ in the visible region largely originates from the S_{16} excitation, which has mixed character of MLCT transitions associated with both the bridging and terminal ligands (HOMO → LUMO+5; HOMO−4 → LUMO +1; HOMO−4 → LUMO+3). The HOMO → LUMO transition is responsible for the low-energy edge absorption of $\mathbf{2}^{2+}$. In the case of the tetraruthenium complex $\mathbf{4}^{4+}$, the predicted MLCT transitions are complex. Three excitations with high oscillator strength in the visible region are predicted (S_8, S_{14}, and S_{24} excitations). They are associated with the HOMO, HOMO−1, HOMO−2, LUMO+2, LUMO+3, LUMO+4, and LUMO+5 orbitals. Apparently, the terminal tpy ligand is not involved in these transitions. Again, the HOMO → LUMO excitation is mainly responsible for its low-energy edge absorption.

Spectroelectrochemical Measurements. The tetrametallic complex $\mathbf{4}^{4+}$ was studied by spectroelectrochemical measurements at a transparent indium−tin oxide (ITO) glass electrode. Figure 9 shows the absorption spectral changes in the visible to NIR region upon a stepwise increase of the potential to oxidize ruthenium sites. When the potential was increased from +0.60 to +0.90 V versus Ag/AgCl, a decrease in the MLCT transitions was observed, with the concomitant emergence of weak absorption between 1200 and 1700 nm (Figure 9a). When the potential was further increased to +1.20 V, the intensity of the MLCT transitions decreased a little further, and the weak absorption in the NIR region decreased as well (Figure 9b). This weak absorption very likely arises from the intervalence charge-transfer (IVCT) transitions among ruthenium sites. However, we did not attempt to quantify an electronic coupling parameter from this weak band, which seems to consist of multiple components judging from the irregular shape. In addition, the presence of multiple metal sites further complicates the situation. Nevertheless, the observation of the IVCT transitions does suggest the presence of electronic interaction among metal sites, which is in accordance with the electrochemical data. This suggests that this complex is potentially useful as a molecular wire.

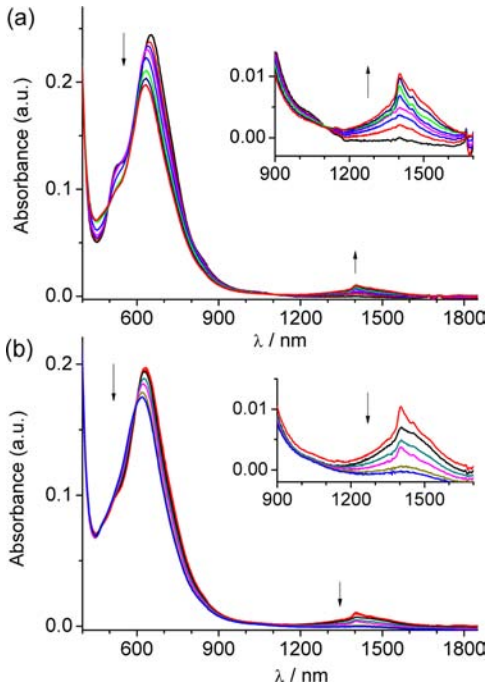

Figure 9. Absorption spectral changes of $\mathbf{4}^{4+}$ in CH_3CN at an ITO glass electrode upon application of potentials from (a) +0.60 to +0.90 V and (b) +0.90 to +1.20 V versus Ag/AgCl. The insets show enlarged plots in the NIR region.

CONCLUSIONS

In summary, the first cyclometalated ruthenium complex with four metal centers has been prepared and characterized using the bridging ligands dpdpz and tppz. It shows enhanced absorptivity and a red-shift absorption maximum compared to the monometallic and dimetallic complexes with dpdpz. Combined electrochemical, spectroscopic, and theoretical studies show that these cyclometalated complexes exhibit intriguing structural and electronic features, including a rigid linear conformation, narrow energy gaps, and low redox potentials of the metal centers. These properties make them potential candidates as molecular wires. Taking into account recent investigations on the photochromic and electrochromic transition-metal complexes with bridged or pendent molecular switch units,[26] these complexes would be of great interest for further elaboration.

On the basis of the theoretical data, we find that the DPDPZ series may be well-suited for molecular electronics applications. The theoretical ΔE_{gap} for the DPDPZ series oligomers is generally narrower than that of the corresponding TPPZ complexes. In shorter oligomers, the presence of a low-lying TPPZ LUMO as well as destabilization of the HOMO from cyclometalation results in a significantly smaller ΔE_{gap}. This may have implications toward the tuning of ΔE_{gap} in future hybrid systems.

EXPERIMENTAL SECTION

Absorption Spectral Measurements. All optical UV−visible absorption spectra were obtained using a HP 8453 diode-array spectrometer at room temperature in denoted solvents, with a conventional 1.0 cm quartz cell. Spectroelectrochemical measurements were performed in a thin-layer cell (optical length 0.2 cm) in which an ITO glass electrode was set in the indicated solvent containing the compound to be studied (the concentration is around 1×10^{-4} M) and 0.1 M Bu_4NClO_4 as the supporting electrolyte. A platinum wire and Ag/AgCl in a saturated aqueous NaCl solution was used as the counter and reference electrodes, respectively. The cell was put into a PE Lambda 750 UV−vis−NIR spectrophotometer to monitor spectral changes during electrolysis.

Electrochemical Measurements. All cyclic voltammetry was taken using an Epsilon BAS EC potentiostat. Three-compartment electrochemical cells (separated by medium-porosity sintered glass disks) with provision for gas addition were employed. All joints were standard taper so that all compartments could be hermetically sealed with Teflon adapters. A glassy carbon electrode with a diameter of 0.3 mm was used as a working electrode. The electrode was polished prior

dx.doi.org/10.1021/ic3019666 | Inorg. Chem. 2012, 51, 13312−13320

to use with 1 μm diamond paste (Buehler) and rinsed thoroughly with water and acetone. A large-area platinum wire coil was used as the counter electrode. All potentials were referenced to a saturated Ag/AgCl electrode without regard for the liquid junction potential. All measurements were carried out with a 0.3 mM concentration of the corresponding complex in CH_3CN at a scan rate of 100 mV/s, in 0.1 M $[^nBu_4N](ClO_4)$ or $[^nBu_4N][B(C_6F_5)_4]$ as the supporting electrolyte.

Synthesis. MALDI-time-of-flight (TOF) positive-ion data were obtained with a Waters MALDI micro MX mass spectrometer run in a reflection mode. The matrix is α-cyano-4-hydroxycinnamic acid. Microanalysis was carried out using a Flash EA 1112 analyzer at the Institute of Chemistry, Chinese Academy of Sciences.

Synthesis of [4](PF$_6$)$_4$. To a suspension of $[Cl_3Ru(tppz)RuCl_3]$[17] (16 mg, 0.02 mmol) in 20 mL of dry acetone was added 52 mg of AgOTf (0.20 mmol). The system was refluxed for 2 h before cooling to room temperature. The mixture was filtered through a pad of Celite, and the filtrate was concentrated under reduced pressure. To the residue were added $[1](PF_6)$[9] (43 mg, 0.05 mmol), 500 mg of 4 Å molecular sieves, 10 mL of DMF, and 10 mL of ^{t}BuOH. The resulting mixture was bubbled with nitrogen for 30 min and then refluxed for 24 h under a nitrogen atmosphere. The mixture was filtered through a pad of Celite, and the filtrate was concentrated. The residue was dissolved in 2 mL of methanol, followed by the addition of excess KPF_6. The resulting precipitate was collected after filtration and subjected to flash column chromatography on silica gel (eluent: CH_3CN/H_2O/aqueous KNO_3, 100:10:5) to give 10 mg of $[4](PF_6)_4$ as a blue solid in 19% yield. MALDI-MS: 2463.4 ($[M - PF_6]^+$), 2317.5 ($[M - 2PF_6]^+$), 2172.6 ($[M - 3PF_6]^+$), 2027.7 ($[M - 4PF_6]^+$). Anal. Calcd for $C_{106}H_{70}F_{24}N_{20}P_4Ru_4{\cdot}2H_2O$: C, 48.15; H, 2.82; N, 10.60. Found: C, 47.94; H, 2.91; N, 10.87.

Computational Methods. In order to minimize the computational cost, rough geometries of all oligomers were generated using the *MOPAC 09* software package and the semiempirical PM6 method, which includes parametrization for 70 elements.[27] Because of its efficient parallelization, the Vienna Ab Initio Simulation Package (VASP) was used to perform geometry optimizations on all DPDPZ and TPPZ oligomers.[28] DFT calculations in VASP used the Perdew–Burke–Ernzerhof form of the generalized gradient approximation.[29,30] Core states were described with a projector augmented-wave pseudopotential, while valence states were expanded on the basis of plane waves with a cutoff energy of 500 eV.[31] Energies were sampled at a single k point, and maximum forces were limited to 0.02 eV/Å. Unit cells were constructed so that a minimum vacuum distance of 15 Å was maintained between periodic images. Where charged species are concerned, VASP employs a homogeneous background charge to achieve charge neutrality in the cell. Electronic structures from the VASP-optimized geometries were calculated using DFT, as implemented in the *Gaussian03* program.[32] Wave functions were expanded in the LANL2DZ basis set with effective core potentials, and an electron exchange correlation was described using the B3LYP hybrid functional.[33,34] Solvation effects in acetonitrile were included using the conductor-like polarizable continuum model with united-atom Kohn–Sham radii.[35]

■ ASSOCIATED CONTENT

Ⓢ Supporting Information

^{1}H NMR spectrum, CV, and DPV curves of 4^{4+}, absorption spectra of 2^{2+}, 4^{4+}, 6^{4+}, and 8^{8+}, DFT and TDDFT results, and optimized Cartesian coordinates of the DPDPZ series. This material is available free of charge via the Internet at http://pubs.acs.org.

■ AUTHOR INFORMATION

Corresponding Author

*E-mail: zhongyuwu@iccas.ac.cn (Y.-W.Z.), hda1@cornell.edu (H.D.A.).

Present Address

[¶]Dupont Central Research and Development, Experiment Station E500/3401a, P.O. Box 80500, Wilmington, DE 19880-0500.

Notes

The authors declare no competing financial interest.

■ ACKNOWLEDGMENTS

Y.-W.Z. thanks the National Natural Science Foundation of China (Grants 21002104, 21271176, and 91227104), the National Basic Research 973 program of China (Grant 2011CB932301), the Scientific Research Foundation for the Returned Overseas Chinese Scholars, State Education Ministry of China, and the Institute of Chemistry, Chinese Academy of Sciences ("100 Talent" Program Grant CMS-PY-201230) for financial support. H.D.A. acknowledges the NSF/CCI phase I award (0847926) for funding support. This work was also supported by Cornell Center for Materials Research. Calculations were performed on the Intel Cluster at the Cornell Nanoscale Facility (CNF) and at the Computational Center for Nanotechnology Innovations at Rensselaer Polytechnic Institute. The Intel Cluster at CNF is a part of the National Nanotechnology Infrastructure Network funded by the National Science Foundation. We are grateful to Prof. Richard G. Hennig of the Department of Materials Science and Engineering at Cornell University for useful discussions.

■ REFERENCES

(1) (a) Diederich, F.; Martin, R. E. *Angew. Chem., Int. Ed.* **1999**, *38*, 1350. (b) Tour, J. M. *Acc. Chem. Res.* **2000**, *33*, 791. (c) Holliday, B. J.; Swager, T. M. *Chem. Commun.* **2005**, 23. (d) Zhao, X.; Zhan, X. *Chem. Soc. Rev.* **2011**, *40*, 3728. (e) Szafert, S.; Gladysz, J. A. *Chem. Rev.* **2006**, *106*, PR1–PR33.

(2) (a) Heeger, A. J. *Chem. Soc. Rev.* **2010**, *39*, 2354. (b) Facchetti, A. *Chem. Mater.* **2011**, *23*, 733. (c) Mishra, A.; Ma, C.-Q.; Bauerle, P. *Chem. Rev.* **2009**, *109*, 1141. (d) Bunz, U. H. F. *Chem. Rev.* **2000**, *100*, 1605. (e) MacDiarmid, A. G. *Angew. Chem., Int. Ed.* **2001**, *40*, 2581. (f) Scherf, U.; List, E. J. W. *Adv. Mater.* **2002**, *14*, 477.

(3) (a) Ho, C.-L.; Wong, W.-Y. *Coord. Chem. Rev.* **2011**, *255*, 2469. (b) Williams, K. A.; Boydston, A. J.; Bielawski, C. W. *Chem. Soc. Rev.* **2007**, *36*, 729. (c) Whittell, G. R.; Hager, M. D.; Schubert, U. S.; Manners, I. *Nat. Mater.* **2011**, *10*, 176.

(4) (a) Ulgut, B.; Abruña, H. D. *Chem. Rev.* **2008**, *108*, 2721. (b) Low, P. J. *Dalton Trans.* **2005**, 2821. (c) Akita, M.; Koike, T. *Dalton Trans.* **2008**, 3523. (d) Tuccitto, N.; Ferri, V.; Cavazzini, M.; Quici, S.; Zhavnerko, G.; Licciardello, A.; Rampi, M. A. *Nat. Mater.* **2009**, *8*, 41. (e) Ying, J.-W.; Liu, I. P.-C.; Xi, B.; Song, Y.; Campana, C.; Zuo, J.-L.; Ren, T. *Angew. Chem., Int. Ed.* **2010**, *49*, 954.

(5) (a) Robert, R. L.; Schwich, T.; Corkery, T. C.; Cifuentes, M. P.; Green, K. A.; Farmer, J. D.; Low, P. J.; Marder, T. B.; Samoc, M.; Humphrey, M. G. *Adv. Mater.* **2009**, *21*, 2318. (b) Ishizuka, T.; Sinks, L. E.; Song, K.; Hung, S.-T.; Nayak, A.; Clays, K.; Therien, M. J. *J. Am. Chem. Soc.* **2011**, *133*, 2884.

(6) (a) Leasure, R. M.; Ou, W.; Moss, J. A.; Linton, R. W.; Meyer, T. J. *Chem. Mater.* **1996**, *8*, 264. (b) Bernhard, S.; Goldsmith, J. I.; Takada, K.; Abruña, H. D. *Inorg. Chem.* **2003**, *42*, 4389. (c) Yao, C.-J.; Zhong, Y.-W.; Nie, H.-J.; Abruña, H. D.; Yao, J. *J. Am. Chem. Soc.* **2011**, *133*, 20720. (d) Yao, C.-J.; Yao, J.; Zhong, Y.-W. *Inorg. Chem.* **2012**, *51*, 6259.

(7) (a) Wong, W.-Y.; Ho, C.-L. *Acc. Chem. Res.* **2010**, *43*, 1246. (b) Padhy, H.; Sahu, D.; Chiang, I.-H.; Patra, D.; Kekuda, D.; Chu, C.-W.; Lin, H.-C. *J. Mater. Chem.* **2011**, *21*, 1196.

(8) (a) Collin, J.-P.; Laine, P.; Launay, J.-P.; Sauvage, J.-P.; Sour, A. *J. Chem. Soc., Chem. Commun.* **1993**, 434. (b) Bolger, J.; Gourdon, A.; Ishow, E.; Launay, J.-P. *J. Chem. Soc., Chem. Commun.* **1995**, 1799. (c) Bonhote, P.; Lecas, A.; Amouyal, E. *Chem. Commun.* **1998**, 885.

(d) Gourdon, A.; Launay, J.-P. *Inorg. Chem.* **1998**, *37*, 5336. (e) Ishow, E.; Gourdon, A.; Launay, J.-P.; Chiorboli, C.; Scandola, F. *Inorg. Chem.* **1999**, *38*, 1504. (f) Duprez, V.; Launay, J.-P.; Gourdon, A. *Inorg. Chim. Acta* **2003**, *343*, 395. (g) Sauers, A. L.; Ho, D. M.; Bernhard, S. *J. Org. Chem.* **2004**, *69*, 8910. (h) Carlson, C. N.; Kuehl, C. J.; Da Re, R. E.; Veauthier, J. M.; Schelter, E. J.; Milligan, A. E.; Scott, B. L.; Bauer, E. D.; Thompson, J. D.; Morris, D. E.; John, K. D. *J. Am. Chem. Soc.* **2006**, *128*, 7230. (i) Singh, S.; de Tacconi, N. R.; Diaz, N. R. G.; Lezna, R. O.; Zuniga, J. M.; Abayan, K.; MacDonnell, F. M. *Inorg. Chem.* **2011**, *50*, 9318.

(9) Zhong, Y.-W.; Wu, S.-H.; Burkhardt, S. E.; Yao, C.-J.; Abruña, H. D. *Inorg. Chem.* **2011**, *50*, 517.

(10) Wu, S.-H.; Burkhardt, S. E.; Yao, J.; Zhong, Y.-W.; Abruña, H. D. *Inorg. Chem.* **2011**, *50*, 3959.

(11) Wu, S.-H.; Abruña, H. D.; Zhong, Y.-W. *Organometallics* **2012**, *31*, 1161.

(12) (a) Yao, C.-J.; Sui, L.-Z.; Xie, H.-Y.; Xiao, W.-J.; Zhong, Y.-W.; Yao, J. *Inorg. Chem.* **2010**, *49*, 8347. (b) Yao, C.-J.; Zhong, Y.-W.; Yao, J. *J. Am. Chem. Soc.* **2011**, *133*, 15697. (c) Shao, J.-Y.; Yang, W.-W.; Yao, J.; Zhong, Y.-W. *Inorg. Chem.* **2012**, *51*, 4343.

(13) (a) Collin, J.-P.; Kayhanian, R.; Sauvage, J.-P.; Calogero, G.; Barigelletti, F.; De Cian, A.; Fischer, J. *Chem. Commun.* **1997**, 775. (b) Coudret, C.; Fraysse, S.; Launay, J.-P. *Chem. Commun.* **1998**, 663. (c) Djukic, J.-P.; Sortais, J.-B.; Barloy, L.; Pfeffer, M. *Eur. J. Inorg. Chem.* **2009**, 817. (d) Jäger, M.; Smeigh, A.; Lombeck, F.; Görls, H.; Collin, J.-P.; Sauvage, J.-P.; Hammarström, L.; Johannsson, O. *Inorg. Chem.* **2010**, *49*, 374. (e) Koivisto, B. D.; Robson, K. C. D.; Berlinguette, C. P. *Inorg. Chem.* **2009**, *48*, 9644. (f) Zhang, Y.-M.; Shao, J.-Y.; Yao, C.-J.; Zhong, Y.-W. *Dalton Trans.* **2012**, *41*, 9280. (g) Yang, W.-W.; Wang, L.; Zhong, Y.-W.; Yao, J. *Organometallics* **2011**, *30*, 2236. (h) Yang, W.-W.; Zhong, Y.-W.; Yoshikawa, S.; Shao, J.-Y.; Masaoka, S.; Sakai, K.; Yao, J.; Haga, M.-a. *Inorg. Chem.* **2012**, *51*, 890.

(14) (a) Wadman, S. H.; Kroom, J. M.; Bakker, K.; Lutz, M.; Spek, A. L.; van Klink, G. P. M.; van Koten, G. *Chem. Commun.* **2007**, 1907. (b) Wadman, S. H.; Kroon, J. M.; Bakker, K.; Havenith, R. W. A.; van Klink, G. P. M.; van Koten, G. *Organometallics* **2010**, *29*, 1569. (c) Robson, K. C. D.; Koivisto, B. D.; Yella, A.; Sporinova, B.; Nazeeruddin, M. K.; Baumgartner, T.; Grätzel, M.; Berlinguette, C. P. *Inorg. Chem.* **2011**, *50*, 5494. (d) Bomben, P. G.; Gordon, T. J.; Schott, E.; Berlinguette, C. P. *Angew. Chem., Int. Ed.* **2011**, *50*, 10682. (e) Kim, J.-J.; Choi, H.; Paek, S.; Kim, C.; Lim, K.; Ju, M.-J.; Kang, H. S.; Kang, M.-S.; Ko, J. *Inorg. Chem.* **2011**, *50*, 11340. (f) Kisserwan, H.; Ghaddar, T. H. *Dalton Trans.* **2011**, *40*, 3877. (g) Funaki, T.; Funakoshi, H.; Kitao, O.; Onozawa-Komatsuzaki, N.; Kasuga, K.; Sayama, K.; Sugihara, H. *Angew. Chem., Int. Ed.* **2012**, *51*, 7528.

(15) (a) Beley, M.; Collin, J.-P.; Louis, R.; Metz, B.; Sauvage, J.-P. *J. Am. Chem. Soc.* **1991**, *113*, 8521. (b) Patoux, C.; Launay, J.-P.; Beley, M.; Chodorowski-Kimmers, S.; Collin, J.-P.; James, S.; Sauvage, J.-P. *J. Am. Chem. Soc.* **1998**, *120*, 3717. (c) Sutter, J.-P.; Grove, D. M.; Beley, M.; Collin, J.-P.; Veldman, N.; Spek, A. L.; Sauvage, J.-P.; van Koten, G. *Angew. Chem., Int. Ed.* **1994**, *33*, 1282. (d) Steenwinkel, P.; Grove, D. M.; Veldman, N.; Spek, A. L.; van Koten, G. *Organometallics* **1998**, *17*, 5647. (e) Gagliardo, M.; Amijs, C. H. M.; Lutz, M.; Spek, A. L.; Havenith, R. W. A.; Hartl, F.; van Klink, G. P. M.; van Koten, G. *Inorg. Chem.* **2007**, *46*, 11133. (f) Fraysse, S.; Coudret, C.; Launay, J.-P. *J. Am. Chem. Soc.* **2003**, *125*, 5880. (g) Vila, N.; Zhong, Y.-W.; Henderson, J. C.; Abruña, H. D. *Inorg. Chem.* **2010**, *49*, 796. (h) Wang, L.; Yang, W.-W.; Zheng, R.-H.; Shi., Q.; Zhong, Y.-W.; Yao, J. *Inorg. Chem.* **2011**, *50*, 7074. (i) Yang, W.-W.; Yao, J.; Zhong, Y.-W. *Organometallics* **2012**, *31*, 1035. (j) Sui, L.-Z.; Yang, W.-W.; Yao, C.-J.; Xie, H.-Y.; Zhong, Y.-W. *Inorg. Chem.* **2012**, *51*, 1590. (k) Yao, C.-J.; Zheng, R.-H.; Shi, Q.; Zhong, Y.-W.; Yao, J. *Chem. Commun.* **2012**, *48*, 5680.

(16) (a) Ruminski, R.; Kiplinger, J.; Cockroft, T.; Chase, C. *Inorg. Chem.* **1989**, *28*, 370. (b) Vogler, L. M.; Scott, B.; Brewer, K. J. *Inorg. Chem.* **1993**, *32*, 898. (c) Arana, C. R.; Abruña, H. D. *Inorg. Chem.* **1993**, *32*, 194. (d) Vogler, L. M.; Brewer, K. J. *Inorg. Chem.* **1996**, *35*, 818. (e) Dattelbaum, D. M.; Hartshom, C. M.; Meyer, T. J. *J. Am. Chem. Soc.* **2002**, *124*, 4938. (f) Chanda, N.; Laye, R. H.; Chakraborty, S.; Paul, R. L.; Jeffery, J. C.; Ward, M. D.; Lahiri, G. K. *J. Chem. Soc., Dalton Trans.* **2002**, 3496. (g) Chanda, N.; Sarkar, B.; Kar, S.; Fiedler, J.; Kaim, W.; Lahiri, G. K. *Inorg. Chem.* **2004**, *43*, 5128. (h) Flores-Torres, S.; Hutchison, G. R.; Stoltzberg, L. J.; Abruña, H. D. *J. Am. Chem. Soc.* **2006**, *128*, 1513.

(17) Hartshom, C. M.; Daire, N.; Tondreau, V.; Loeb, B.; Meyer, T. J.; White, P. S. *Inorg. Chem.* **1999**, *38*, 3200.

(18) (a) Geiger, W. E.; Barrière, F. *Acc. Chem. Res.* **2010**, *43*, 1030. (b) LeSuer, R. J.; Geiger, W. E. *Angew. Chem., Int. Ed.* **2000**, *39*, 248. (c) Barrière, F.; Geiger, W. E. *J. Am. Chem. Soc.* **2006**, *128*, 3980. (d) Hildebrandt, A.; Schaarschmidt, D.; Lang, H. *Organometallics* **2011**, *30*, 556.

(19) LeSuer, R.; Bettolph, C.; Geiger, W. E. *Anal. Chem.* **2004**, *76*, 6395.

(20) Fantacci, S.; De Angelis, F.; Wang, J. J.; Bernhard, S.; Selloni, A. *J. Am. Chem. Soc.* **2004**, *126*, 9715.

(21) Zhao, S.; Archchige, S. M.; Slebodnick, C.; Brewer, K. J. *Inorg. Chem.* **2008**, *47*, 6144.

(22) Wadman, S. H.; Lutz, M.; Tooke, D. M.; Spek, A. L.; Hartl, F.; Havenith, R. W. A.; van Klink, G. P. M.; van Koten, G. *Inorg. Chem.* **2009**, *48*, 1887.

(23) Parr, R. G.; Pearson, R. G. *J. Am. Chem. Soc.* **1983**, *105*, 7512.

(24) (a) Martin, R. E.; Gubler, U.; Boudon, C.; Gramlich, V.; Bosshard, C.; Gisselbrecht, J.-P.; Günter, P.; Gross, M.; Diederich, F. *Chem.—Eur. J.* **1997**, *3*, 1505. (b) Monkman, A. P.; Burrows, H. D.; Hamblett, I.; Navarathnam, S.; Svensson, M.; Andersson, M. R. *J. Chem. Phys.* **2001**, *115*, 9046. (c) Izumi, T.; Kobashi, S.; Takimiya, K.; Aso, Y.; Otsubo, T. *J. Am. Chem. Soc.* **2003**, *125*, 5286. (d) Rissler, J. *Chem. Phys. Lett.* **2004**, *395*, 92. (e) Tsuda, A.; Osuka, A. *Science* **2001**, *293*, 79.

(25) Seminario, J. M.; Zacarias, A. G.; Tour, J. M. *J. Am. Chem. Soc.* **2000**, *122*, 3015.

(26) (a) Zhong, Y.-W.; Vila, N.; Henderson, J. C.; Flores-Torres, S.; Abruña, H. D. *Inorg. Chem.* **2007**, *46*, 10470. (b) Zhong, Y.-W.; Vila, N.; Henderson, J. C.; Abruña, H. D. *Inorg. Chem.* **2009**, *48*, 991. (c) Zhong, Y.-W.; Vila, N.; Henderson, J. C.; Abruña, H. D. *Inorg. Chem.* **2009**, *48*, 7080. (d) Kume, S.; Nishihara, H. *Dalton Trans.* **2008**, 3260. (e) Kume, S.; Nishihara, H. *Struct. Bonding* **2007**, *123*, 79.

(27) Stewart, J. J. P. *J. Mol. Model.* **2007**, *13*, 1173.

(28) (a) Kresse, G.; Hafner, J. *J. Phys. Rev. B* **1993**, *47*, 558. (b) Kresse, G.; Furthmüller, J. *Comput. Mater. Sci.* **1996**, *6*, 15. (c) Kresse, G.; Furthmüller, J. *J. Phys. Rev. B* **1996**, *54*, 11 169. (d) Kresse, G.; Joubert, D. *Phys. Rev. B* **1999**, *59*, 1758.

(29) Kohn, W.; Sham, L. *J. Phys. Rev. A* **1964**, *140*, 1133.

(30) (a) Perdew, J. P.; Burke, K.; Ernzerhof, M. *Phys. Rev. Lett.* **1996**, *77*, 3865. (b) Perdew, J. P.; Burke, K.; Ernzerhof, M. *Phys. Rev. Lett.* **1997**, *78*, 1396 (erratum)..

(31) Blöchl, P. E. *Phys. Rev. B* **1994**, 50, *17* 953

(32) Frisch, M. J.; Trucks, G. W.; Schlegel, H. B.; Scuseria, G. E.; Robb, M. A.; Cheeseman, J. R.; Montgomery, J. A., Jr.; Vreven, T.; Kudin, K. N.; Burant, J. C.; Millam, J. M.; Iyengar, S. S.; Tomasi, J.; Barone, V.; Mennucci, B.; Cossi, M.; Scalmani, G.; Rega, N.; Petersson, G. A.; Nakatsuji, H.; Hada, M.; Ehara, M.; Toyota, K.; Fukuda, R.; Hasegawa, J.; Ishida, M.; Nakajima, T.; Honda, Y.; Kitao, O.; Nakai, H.; Klene, M.; Li, X.; Knox, J. E.; Hratchian, H. P.; Cross, J. B.; Bakken, V.; Adamo, C.; Jaramillo, J.; Gomperts, R.; Stratmann, R. E.; Yazyev, O.; Austin, A. J.; Cammi, R.; Pomelli, C.; Ochterski, J. W.; Ayala, P. Y.; Morokuma, K.; Voth, G. A.; Salvador, P.; Dannenberg, J. J.; Zakrzewski, V. G.; Dapprich, S.; Daniels, A. D.; Strain, M. C.; Farkas, O.; Malick, D. K.; Rabuck, A. D.; Raghavachari, K.; Foresman, J. B.; Ortiz, J. V.; Cui, Q.; Baboul, A. G.; Clifford, S.; Cioslowski, J.; Stefanov, B. B.; Liu, G.; Liashenko, A.; Piskorz, P.; Komaromi, I.; Martin, R. L.; Fox, D. J.; Keith, T.; Al-Laham, M. A.; Peng, C. Y.; Nanayakkara, A.; Challacombe, M.; Gill, P. M. W.; Johnson, B.; Chen, W.; Wong, M. W.; Gonzalez, C.; Pople, J. A. *Gaussian03*, revision E.01; Gaussian, Inc.: Wallingford, CT, 2004.

(33) (a) Dunning, T. H.; Hay, P. J. In *Modern Theoretical Chemistry*; Schaefer, H. F., Ed.; Plenum: New York, 1976; Vol. 3, p 1. (b) Hay, P.

J.; Wadt, W. R. *J. Chem. Phys.* **1985**, *82*, 270. (c) Wadt, W. R.; Hay, P. J. *J. Chem. Phys.* **1985**, *82*, 284. (d) Hay, P. J.; Wadt, W. R. *J. Chem. Phys.* **1985**, *82*, 299.
(34) (a) Becke, A. D. *J. Chem. Phys.* **1993**, *98*, 5648. (b) Lee, C.; Yang, W.; Parr, R. G. *Phys. Rev. B* **1988**, *37*, 785.
(35) (a) Klamt, A.; Schüürmann, G. *J. Chem. Soc., Perkin Trans. 2* **1993**, 799. (b) Andzelm, J.; Kölmel, C.; Klamt, A. *J. Chem. Phys.* **1995**, *103*, 9312. (c) Barone, V.; Cossi, M. *J. Phys. Chem. A* **1998**, *102*, 1995. (d) Cossi, M.; Rega, N.; Scalmani, G.; Barone, V. *J. Comput. Chem.* **2003**, *24*, 669. (e) Takano, Y.; Houk, K. N. *J. Chem. Theory Comput.* **2005**, *1*, 70.